

# Numerical study on ULF waves in a dipole field excited by sudden impulse

YANG Biao<sup>1</sup>, FU SuiYan<sup>1†</sup>, ZONG QiuGang<sup>1,2</sup>, WANG YongFu<sup>1</sup>, ZHOU XuZhi<sup>1</sup>, PU ZuYin<sup>1</sup> & XIE Lun<sup>1</sup>

<sup>1</sup> Institute of Space Physics and Applied Technology, Peking University, Beijing 100871, China;

<sup>2</sup> Center for Atmospheric Research, University of Massachusetts Lowell, Lowell, MA 01854-3629, USA

A three-dimensional numerical model is employed to investigate ULF waves excited by the sudden impulse (SI) of the solar wind dynamic pressure interacting with a dipole magnetosphere. We focus on the solar wind-magnetosphere energy coupling through ULF waves, and the influences of the SI spectrum on the cavity mode structure and the energy deposition due to field line resonances (FLRs) in the magnetosphere. The numerical results show that for a given SI lasting for 1 min with amplitude of 50 mV/m impinging on the subsolar magnetopause, the total ULF energy transported from the solar wind to the magnetosphere is about the magnitude of  $10^{14}$  J. The efficiency of the solar wind energy input is around 1%, which depends little on the location of the magnetopause in the model. It is also found that the energy of the cavity mode is confined in the region near the magnetopause, whereas, the energy of the toroidal mode may be distributed among a few specific *L*-shells. With a given size of the model magnetosphere and plasma density distribution, it is shown that the fundamental eigenfrequency of the cavity mode and the central locations of the FLRs do not vary noticeably with the power spectrum of the SI. It is worth noting that the spectrum of the SI affects the excitation of higher harmonics of the global cavity mode. The broader the bandwidth of the SI is, the higher harmonics of cavity mode could be excited. Meanwhile, the corresponding FLRs regions are broadened at the same time, which implies that the global cavity modes and toroidal modes can resonate on more magnetic *L*-shells when more harmonics of the global cavity modes appear.

sudden impulse, ULF waves, global cavity mode, toroidal mode, field line resonances

## 1 Introduction

The Ultra Low Frequency (ULF) waves are geomagnetic pulsations with frequency from 1 mHz to

Received January 7, 2008; accepted July 15, 2008

doi: 10.1007/s11431-008-0251-1

<sup>†</sup>Corresponding author (email: [suiyanfu@pku.edu.cn](mailto:suiyanfu@pku.edu.cn))

Supported by the National Natural Science Foundation of China (Grant Nos. 40425004 and 40528005) and the Major State Basic Research Development Program of China (973 Program) (Grant No. 2006CB806305)

1 Hz. It is generally believed that the ULF waves are excited by either the external solar wind disturbance or the internal plasma instabilities in the magnetosphere and are playing an important role in the solar wind-magnetosphere energy coupling.

The Magnetohydrodynamic (MHD) waves in the uniform cold plasma are characterized by two decoupled types called shear Alfvén wave and fast compressional wave. The shear Alfvén wave propagates along the magnetic field lines. If we assume that the ends of the field line are fixed at conjugating ionospheres, field line resonance occurs when the external driving frequency matches the eigenfrequency of the Alfvén wave. On the other hand, the compressional wave propagates across the magnetic field lines. The global cavity resonance may be excited when the fast compressional wave reflects back and forth in the magnetospheric cavity with boundaries having great plasma density gradients, such as the magnetopause and plasmapause. It is the sizes of the magnetospheric cavity and the plasma density distributions that determine the eigenfrequencies of the global cavity modes. These two modes always couple with each other in the inhomogeneous plasma<sup>[1]</sup>.

The three components of the magnetic field represent three different kinds of ULF modes in the mean field-aligned coordinate. The field-aligned magnetic field perturbation is called compressional mode, while the transverse perturbations are identified as toroidal mode and poloidal mode<sup>[2]</sup>. The toroidal mode consists of azimuthal magnetic field and radial electric field disturbance and corresponds to the characteristic of the shear Alfvén wave. The poloidal mode consists of radial magnetic field and azimuthal electric field disturbance. It will cause the interaction of adjacent magnetic shell due to the different eigenfrequencies and change the magnetic field intensity, so it appears partly as the characteristics of fast compressional wave.

The mechanism of how the field line resonance (FLR) of standing Alfvén waves is excited has been studied for decades. The earliest “steady-state driving” model<sup>[3,4]</sup> took emphasis on the successive monochromatic surface waves excited by the Kelvin-Helmholtz instability on the magnetopause. They could drive FLRs where the eigenfrequency of the local standing Alfvén waves matches the frequency of these surface waves. This model successfully explained the ULF pulsation phenomenon observed on the ground, such as frequency variation with latitude and polarization reversal across the magnetic noon meridian<sup>[5]</sup>. However, the discrete spectra of ULF pulsations were usually observed and could not be well explained<sup>[6]</sup>. Later work by Kivelson<sup>[7,8]</sup> speculated the cavity mode induced by a broad-band source (e.g. the solar wind dynamic pressure pulse). In this scenario, the cavity modes with discrete spectra were first produced in the magnetosphere and then resonated with the Alfvén standing waves at different  $L$  shells respectively. Numerous numerical works presented extensive evidence of the cavity mode and its coupling to the local Alfvén standing wave<sup>[9–12]</sup>. Since the magnetosphere is open downtail along which the fast mode may disperse, further studies<sup>[13–17]</sup> suggested that the waveguide model was more realistic in the frank and tail region of the magnetosphere than cavity model. The waveguide mode could be excited either by the solar wind dynamic impulse<sup>[18]</sup> or the high speed flows in the frank of the magnetopause<sup>[19]</sup>. Mann<sup>[19]</sup> suggested that the waveguide mode could be energized by the high speed magnetosheath flows in the frank region due to an over reflection mechanism. Whereas, the magnetopause around noon, where the stagnation of the magnetosheath flows gave rise to a leaky boundary, was unable to trap waveguide modes effectively. In addition, other surveys showed that the FLRs could be directly driven by solar wind perturbations<sup>[20–22]</sup>.

There are few studies concerning the energy of the ULF waves. Greenwald<sup>[23]</sup> showed a Pc5 toroidal pulsation observed by STARE radar. The total energy of ULF dissipation via Joule heating

was about  $2 \times 10^{13}$  J, comparable to the energy dissipated in the ionosphere by Joule heating during a small substorm. Crowley<sup>[24]</sup> presented another Pc5 pulsation event caused by the solar wind dynamic pressure pulse. Using both the EISCAT radar and ground-based magnetometers, he indicated that the total energy dissipated in the ionosphere by this pulsation was  $4 \times 10^{12}$  J. However, the global picture of the ULF energy transported from the solar wind to the magnetosphere remains unclear. Although multi-satellite observations are widely utilized to study ULF waves<sup>[25,26]</sup>, it is still not capable of getting the global energy distribution of the ULF pulsations, especially for the compressional mode. Even though the ULF energy distribution in the magnetosphere could be obtained by vasty ground-based radar and magnetometer chains, the ULF waves propagating to the ground have been intensively affected by ionosphere currents (e.g. change the polarization of the Alfvén waves due to an ionospheric screening effect<sup>[27]</sup>). In addition, they may also be attenuated due to the finite conductivities of the ionosphere<sup>[28]</sup>.

Recently the ULF pulsations are supposed to accelerate relativistic electrons in the outer radiation belt effectively. Elkington<sup>[29]</sup> showed in his numerical study that the Pc5 band toroidal mode could successively accelerate the electrons via drift resonance. Zong<sup>[30]</sup> presented an *in-situ* Cluster observation of energetic particle flux modulated by the ULF wave in the dayside magnetosphere during the recovery phase of the Halloween storm on Oct. 31, 2003. They claimed that the periodical variation of the electron flux observed by Cluster is due to drift resonance between the ULF toroidal mode and the electrons with energy of around 127 keV. In fact, the global energy distribution of the ULF waves not only is essential to the process of solar wind-magnetosphere energy coupling, but also important to revealing the details of the wave-particle interactions in the inner magnetosphere.

Lee and Lysak<sup>[12]</sup> studied the spatial structure and the coupling effect of the ULF waves excited by the solar wind pressure impulse in a two-dimensional dipole model, and they also developed this model to a three-dimensional one<sup>[31]</sup>. In this study, based on the model of Lee and Lysak<sup>[31]</sup>, we focus on the solar wind-magnetosphere energy coupling through the ULF waves, and the influences of the SI spectrum on the cavity mode structure as well as the energy deposition due to the FLRs in the magnetosphere.

## 2 Numerical model

We use the dipole model of Lee and Lysak<sup>[12,31]</sup>. The following linear equations can be derived from the ideal MHD and Maxwell equations if the cold plasma is considered:

$$\begin{cases} \frac{\partial \mathbf{B}_1}{\partial t} = -\nabla \times \mathbf{E}_1, \\ \frac{\partial \mathbf{E}_1}{\partial t} = V_a^2 (\nabla \times \mathbf{B}_1)_\perp, \end{cases} \quad (1)$$

where  $V_a$  is the Alfvén velocity. We adopt the dipole coordinate<sup>[31]</sup>  $(\mu, \nu, \varphi)$ , and attain the Lamé factors corresponding to the spherical coordinate  $(r, \theta, \varphi)$ :

$$\begin{aligned} \mu &= \frac{\sin \theta}{r^2}, & h_\mu &= \frac{r^3}{\sqrt{1 + 3 \sin^2 \theta}}, \\ \nu &= -\frac{\cos^2 \theta}{r}, & h_\nu &= \frac{r^2}{\cos \theta \sqrt{1 + 3 \sin^2 \theta}}, \end{aligned}$$

$$\boldsymbol{\varphi} = \varphi, \quad h_\varphi = r \cos \theta,$$

where  $\boldsymbol{\mu}$ ,  $\boldsymbol{v}$ ,  $\boldsymbol{\varphi}$  are field-aligned, radial, and azimuthal vectors respectively in the dipole coordinate;  $\theta$  is the magnetic latitude; and  $r$  is the geocentric radius vector. The dipole magnetic field is given by

$$B(r, \theta) = B_0 \frac{R_E^3}{r^3} \sqrt{1 + 3 \sin^2 \theta},$$

$B_0$  is the equatorial magnetic field on the Earth's surface (31000 nT).  $R_E$  is the radius of the Earth. We use the plasma density model derived by Singer<sup>[32]</sup>:

$$n(r) = n_{\text{eq}}(L) \left( \frac{R_E L}{r} \right)^6, \quad n_{\text{eq}}(L) = n_0 \left( \frac{r_{\text{mp}}}{R_E L} \right)^3,$$

where  $r_{\text{mp}}$  and  $n_0$  are the distance and number density of the magnetopause, respectively. Assume  $r_{\text{mp}} = 10 R_E$ ,  $n_0 = 0.5 \text{ cm}^{-3}$ .

The relation of  $r$  and  $L$  is determined by  $r^2 = L R_E \cos^2 \theta$ , where  $L$  is the distance from the center of the Earth to the point where a magnetic field line crosses the equator, measured in Earth radii. Since the magnetic field and the plasma density distribution are determined, the Alfvén velocity is obtained as follows:

$$V_a(r, \theta) = \frac{B^2(r, \theta)}{\sqrt{\mu_0 m_p n(r)}},$$

where  $\mu_0$  is the vacuum permeability,  $m_p$  is the proton mass.

The plasmapause (4.5  $R_E$ ) and the magnetopause (10  $R_E$ ) are selected as the inner and outer boundaries in the model, and the ionosphere has a geocentric distance of 2  $R_E$ . Just as what Lee and Lysak<sup>[12]</sup> did, we assume the plasmapause to be perfect reflector and the ionosphere to be an ideal conductor.

An azimuthal component of electric field is assumed to represent the effect of the solar wind sudden impulse without distortion of the geometry of the grids. The time and space dependence of  $E_\varphi$  are given as follows<sup>[33]</sup>:

$$\begin{aligned} E_\varphi|_{\text{boundary}} &= A_{\text{time}} A_{\text{space}}, \\ A_{\text{time}} &= k_3 (t - 0.5 t_{\text{max}}) \exp \left[ - \left( k_4 \frac{t - 0.5 t_{\text{max}}}{t_{\text{max}}} \right)^2 \right], \\ A_{\text{space}} &= \exp \left[ - \left( k_1 \frac{\mu}{\mu_{\text{max}}} \right)^2 \right] \exp \left[ - \left( k_2 \frac{\varphi}{\varphi_{\text{max}}} \right)^2 \right], \end{aligned}$$

where  $k_1$ ,  $k_2$ ,  $k_3$ ,  $k_4$  and  $t_{\text{max}}$  are the adjustable parameters. Here,  $t_{\text{max}}$  is the time duration of the impulse;  $k_1$  and  $k_2$  control the magnitude of the space dependence of impulse in the field-aligned and azimuthal directions respectively;  $k_3$  and  $k_4$  control the amplitude and spectrum of the impulse in time dependence respectively. Figure 1 shows an example of the impulse. It has a time profile (Figure 1(a)) of 1 min duration and a peak-peak value of 50 mV/m, and spatial distribution (Figure 1(b)) with attenuation in both the field-aligned and azimuthal directions from the subsolar magnetopause. The values of the controlling parameters are given in the figure for detail.

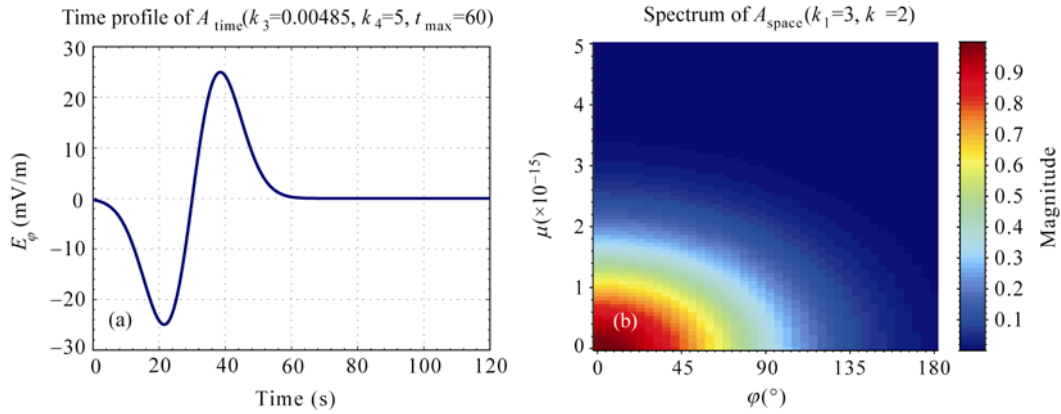


**Figure 1** The time profile (a) and the spatial distribution (b) of the given sudden impulse at the outer boundary of the magnetopause.

### 3 Results

#### 3.1 Total energy of the ULF waves and energy distribution of different modes

We first consider the total energy of the ULF waves in the magnetosphere excited by the sudden impulse as given in Figure 1. The energy density of each grid is determined by

$$w = \frac{1}{2\mu_0} \left( B_1^2 + \frac{E_1^2}{V_a^2} \right).$$

The total energy could be obtained by integrating all the grids. Figure 2 gives the time profile of the total energy in the foremost 400 s. Since there is no energy dissipation in the model, the total energy is about  $1.1 \times 10^{14}$  J when the system reaches its quasi-steady state.

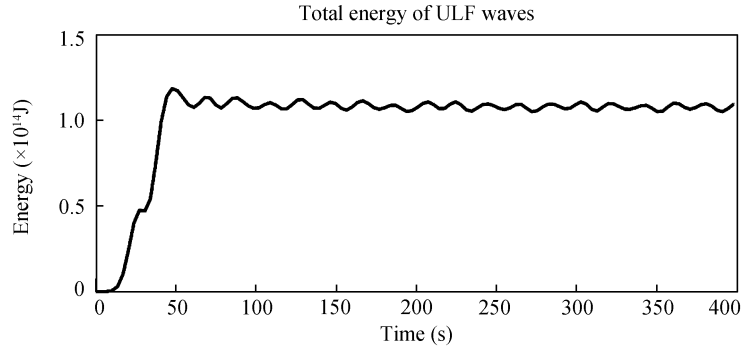


**Figure 2** The time profile of the total ULF energy in the magnetosphere.

Figure 3 shows the evolution of the radial energy distribution of the global cavity mode (a) and toroidal mode (b). The energy of the cavity mode is confined in the region near the magnetopause, whereas, the energy of the toroidal mode is distributed among a few specific  $L$ -shells. It is shown that the field line resonances occur where the toroidal energy deposits. We can find two FLRs regions with centric location around  $L=5.18$ ,  $7.40$ , and the strongest FLR occurs on  $L=5.18$ .

Southwood<sup>[4]</sup> showed that in the box model there existed a turning point of the compressional wave due to the inhomogeneous plasma or magnetic field. The compressional wave oscillated in the region between the outer boundary and the turning point and became evanescent once across

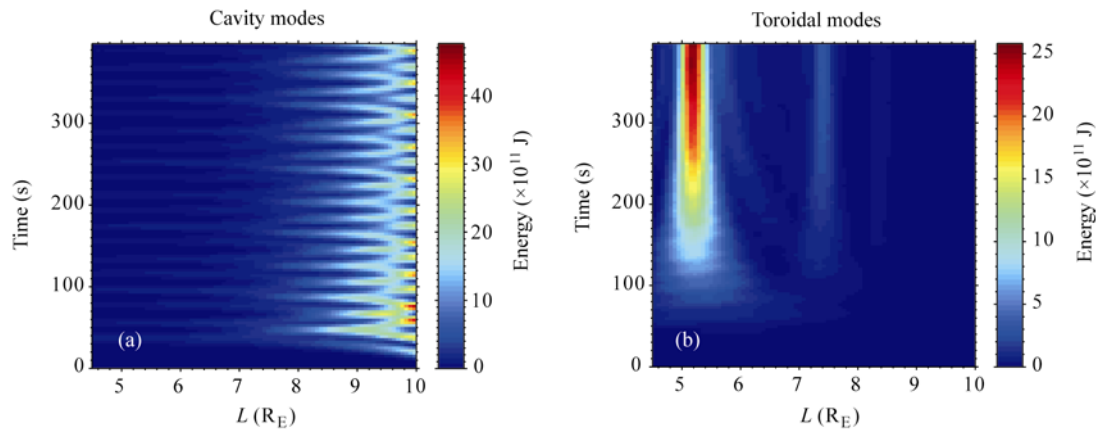


**Figure 3** Energy distribution of cavity mode (a) and toroidal mode (b) depends on  $L$  value and time.

the turning point. The turning point could be distinct for different cavity mode harmonics. In addition, a coupling point existed in the evanescent region. The dispersion relation of the compressional wave was identical to the standing Alfvén wave right at this point, so that FLRs occur via the irreversible energy conversion from the fast compressional wave into the shear Alfvén wave. The numerical results shown in Figure 2 are well consistent with this scenario. We can estimate that the turning point is located on  $L=8.20$ . Two coupling points can be found with centric location on  $L=5.18, 7.40$ . We attribute the different turning points to the coupling of different harmonics of cavity modes with toroidal modes. Obviously, the turning points are located in the evanescent region ( $4.5 < L < 8.2$ ).

### 3.2 Influences of the SI spectrum on the cavity mode structure and energy deposition of FLRs

In order to know how the spectra of the sudden impulse influence the cavity mode structure and the energy deposition due to FLRs, we conducted several experiments with different impulses. Figures 4(a)–4(c) show the time profiles of three impulses with the same peak-peak value (50 mV/m) and different time durations which are 30, 60, 90 s, respectively. Figures 4(d)–4(f) present the corresponding power spectrum density distribution. It is obvious that the peak frequency and band width of the spectrum are different from each other. We can get the peak frequencies: (a)  $f_m=38$  mHz, (b)  $f_m=18$  mHz, (c)  $f_m=12$  mHz, and corresponding band width of 34, 24, 15 mHz, if we define the full width at the half maximum.

A set of grid points are selected along a constant  $\mu$  in the dayside magnetosphere near the equator plane (see Figure 1, and ref. [12]). FFT analysis is applied to  $B_\mu$  of these grids in order to examine the cavity mode structures. As shown in (a), (b), (c) of Figure 5, the first peak of the cavity mode power spectrum density appears on  $f=25$  mHz in spite of the spectrum of the impulse. However, it is uncertain whether this frequency is the fundamental frequency of the global cavity mode. In a simplified scenario, Heddal<sup>[33]</sup> assumed a one-dimensional box model with boundaries at  $4.5 R_E$  and  $10 R_E$  respectively. The dipole magnetic field in the equatorial plane and the plasma density model in equatorial plane in section 2 are applied in this simplified model to get the analytical results of eq. (1), in which the first five harmonics of the cavity modes are 22.17, 45.17, 68.06, 90.90, 113.72 mHz, respectively. Based on his results, we could infer that 25 mHz where the first peak power spectral density appears is just the fundamental frequency of the cavity mode.

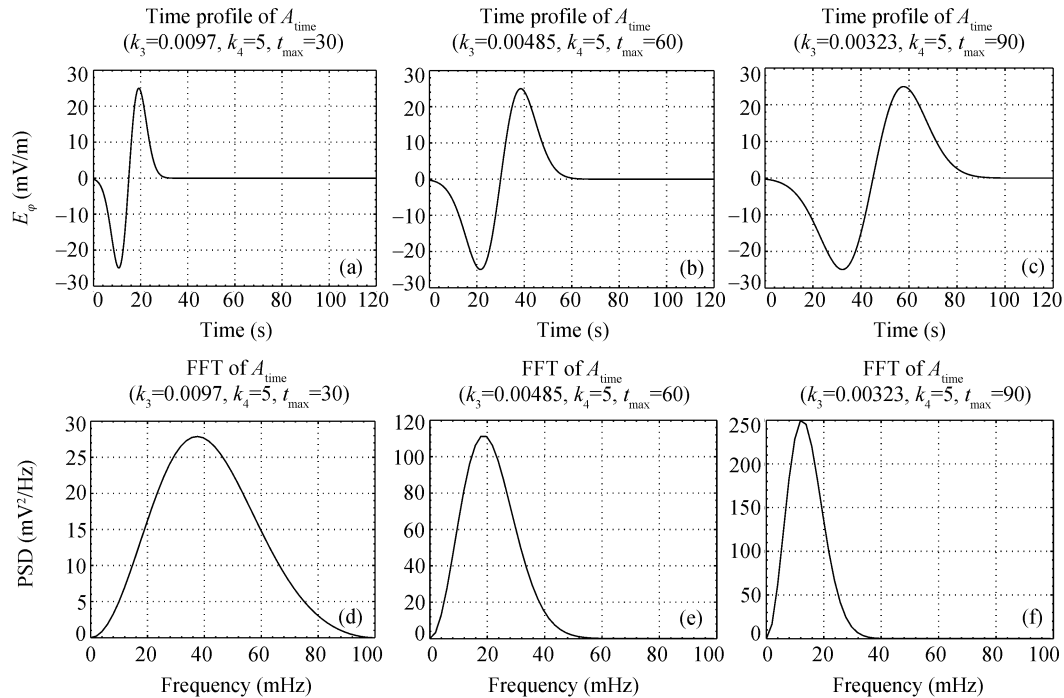


**Figure 4** The time profiles of the impulses with different time width (a)–(c) and the corresponding power spectrum density distribution profiles (d)–(f).

In addition, it is shown that the broader the bandwidth of the impulse is, the higher harmonics of cavity mode are excited. To make it more clear, we extracted the spectrum profile at  $L=6$ , as shown in Figure 6. The power spectrums of the cavity modes excited by different impulses are given in logarithm. The dashed lines of each panel indicate the harmonics. For the impulse with the narrowest bandwidth (Figure 6(c)), we could merely see the fundamental mode (25 mHz). The second harmonic (50 mHz) appears corresponding to the impulse with moderate band width (Figure 6(b)). When the band width of the impulse becomes even broader, the third (70 mHz) and the fourth (103 mHz) harmonics occur obviously. Although the eigenfrequencies of the cavity modes are determined by the intrinsic characteristics of the magnetosphere cavity (we can convince this speculation from the unchanging fundamental frequency), it is implied that the spectrum of the impulse could prominently affect the excitation of the higher harmonics of the global cavity mode.

We examined the regions of the FLRs according to the toroidal energy distribution. Figures 5(d), (e) and (f) display the dependence of the normalized toroidal energy distribution on  $L$  values corresponding to the impulse with duration of 30, 60, 90 s, respectively. It shows that the centric locations of the FLRs do not vary noticeably with different impulse. However, the energy deposition regions could be more dispersed as shown in Figure 5(d) due to the broader spectrum of the driving impulse. For inhomogeneous plasma, the large amplitude FLRs occur due to the irreversible energy conversion from the global cavity mode to the toroidal mode when the frequency of the cavity mode is consistent with the local standing Alfvén wave<sup>[11]</sup>. The relative broader band impulse excites more cavity mode harmonics and would inevitably stimulate the FLRs on more magnetic shells, and therefore leading to the energy dispersion of the toroidal mode.



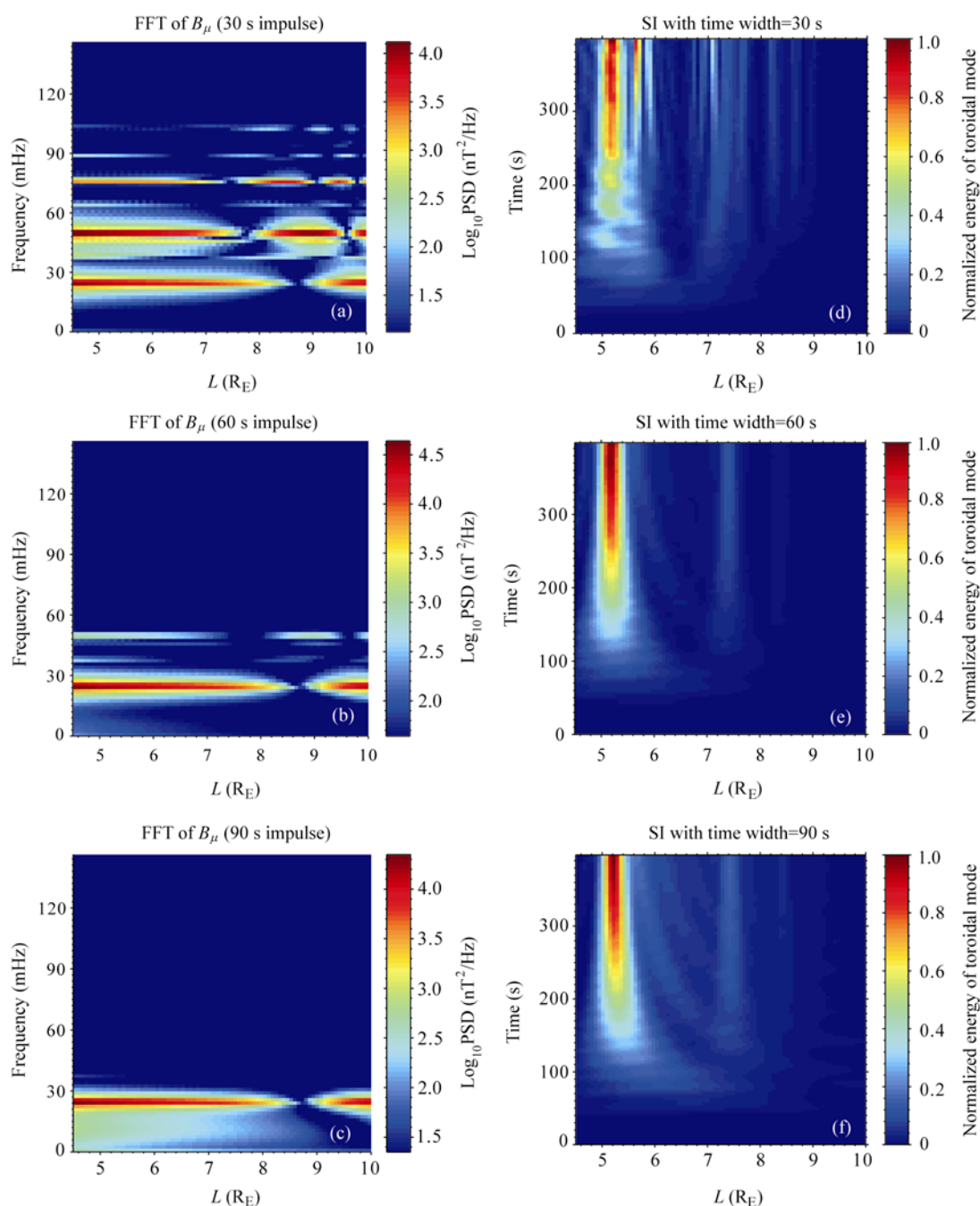


**Figure 5** The power spectrum distribution of cavity mode along a constant  $\mu$ , (a)–(c) correlated to the response of the impulses with time durations of 30, 60, 90 s respectively and the corresponding energy distribution of the toroidal mode (d)–(f).

## 4 Discussion

Using the dipole model developed by Lee and Lysak<sup>[31]</sup>, we quantitatively investigated the energy transport process from the solar wind to the magnetosphere in terms of the ULF waves during the sudden impulse stimulation. For a given impulse lasting for 1 min with amplitude of 50 mV/m



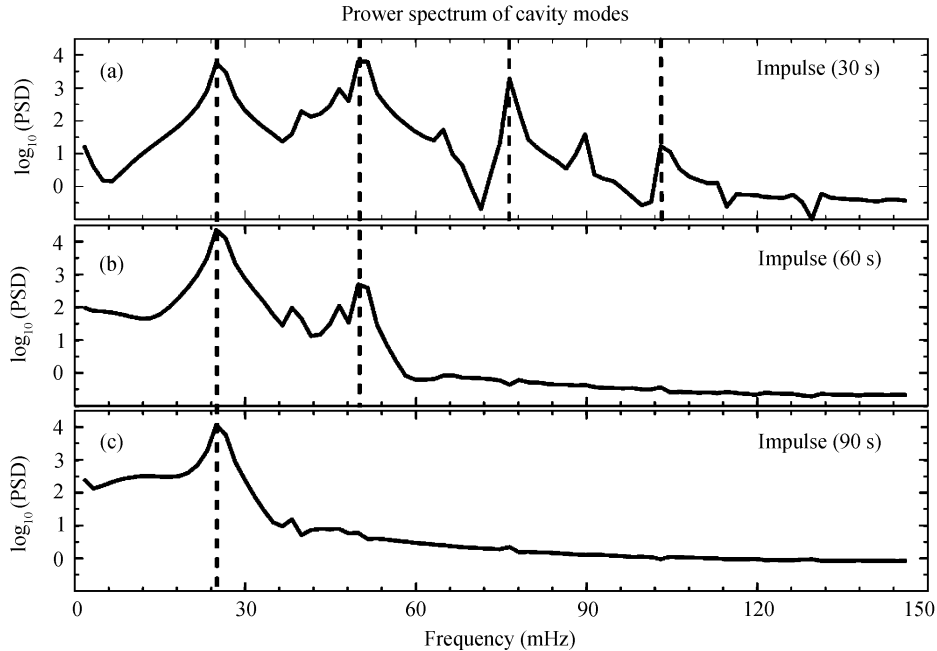


**Figure 6** The power spectrum profile of cavity mode at  $L=6$  of the constant  $\mu$ , (a), (b), (c) are correlated to the impulses with time width of 30, 60, 90 s, respectively.

impinging on the subsolar magnetopause, the total ULF energy transported from the solar wind to the magnetosphere was about  $1.1 \times 10^{14}$  J. The efficiency of the solar wind energy input is about 1.24%. In order to estimate the effect of the magnetopause location on the quantitative result, we set the magnetopause on  $9 R_E$  and  $11 R_E$  respectively with the driving impulse in section 3.1 unchanged. The total ULF energy is  $0.48 \times 10^{14}$  J and total solar wind energy input is  $3.99 \times 10^{15}$  J when the magnetopause is located on  $9 R_E$ , with an energy transport efficiency of 1.20%; if we put the magnetopause at  $11 R_E$ , the total ULF energy and solar wind energy input are  $1.87 \times 10^{14}$  J and  $18.2 \times 10^{15}$  J, respectively and energy transport efficiency is 1.03%. It is obvious that the efficiency of the solar wind energy transportation is around 1% in spite of the location of the magnetopause in the model, though the total ULF energy shows some differences.

It is widely accepted that magnetic reconnection is the predominant process in the solar wind-magnetosphere energy coupling, especially during substorms. Tanskanen<sup>[34]</sup> has presented a statistical survey of solar wind energy input during substorms. For an isolated substorm, the medium energy transported from solar wind to the magnetosphere is about  $1.4 \times 10^{15}$  J, and the energy dispersed by Joule heating in the ionosphere is about  $0.4 \times 10^{15}$  J. Although the total energy derived from our model is not as much as the one during a substorm, the energy carried by the ULF waves may be still considerable.

The radial energy distributions of different modes reveal that the cavity mode energy is confined in the region near the magnetopause, corresponding to the high latitude region of the Earth. However, the energy could penetrate to the lower latitude carried by the toroidal mode due to the coupling effect. We can see the occurrence of the strongest FLRs on  $L=5.18$ , corresponding to the invariable latitude of  $64^\circ$ .

Wygant<sup>[35]</sup> showed an electric field disturbance with magnitude of 80 mV/m observed by

CRRES in the inner magnetosphere during the storm sudden commencement on March 24, 1991. The electric field on the magnetopause is derived to be approximately 200–300 mV/m. It is demonstrated from this study that the impulse with amplitude of 50 mV/m is reasonable in reality during intensive geomagnetic activities.

The numerical results here indicate that fundamental frequency of the global cavity mode is identical despite of the external driving impulse. However, this fundamental frequency would change if the plasma density distribution varies in the magnetosphere. Goldstein<sup>[36]</sup> applied a half-empirical plasma density distributions based on Polar observation to the dipole model of Lee and Lysak<sup>[12]</sup>. His numerical result showed that the fundamental frequency of the cavity mode is 3.5 mHz, which was well consistent with the Polar *in-situ* observations. The ULF pulsations observed by Cluster constellation in the dayside magnetosphere during the solar wind pressure pulse were presented by Eriksson<sup>[37]</sup>. In his study, two different harmonics were revealed with one at 6.8 mHz and another at 27 mHz. He speculated that the tailward propagating cavity/waveguide modes were stimulated by the pressure impulse and these eigen modes in turn couple to the toroidal and poloidal standing wave modes. Comparison of the numerical study with the observations is needed in further study in order to reveal the global properties of the ULF waves excited by the sudden impulse more effectively.

As expected, the central locations of the FLRs do not vary noticeably. We believe that it comes directly from the coupling of the cavity modes and toroidal waves. More interestingly, we have found that the impulse with relatively broad spectrum may excite more harmonics of the cavity mode, which implied that the spectrum of the impulse could prominently affect the excitation of the higher harmonics of the global cavity mode. When the higher harmonics appear, the regions of the FLRs are broadened. We speculate that more cavity mode harmonics would stimulate the FLRs on more magnetic shells, which will cause the toroidal energy dispersion. Lee<sup>[38]</sup> investigated the effects of ionospheric damping on the ULF wave mode structure and suggested that the locations of field line resonances spread wider as the ionospheric damping increased. It is demonstrated that the regions of the FLRs may be influenced by the spectrum characteristic of the driving impulse as well as the ionosphere damping. Since the amplitude of each impulse is identical to another, it is reasonable to fix the location of the magnetopause in the numerical model. If we change the location of the magnetopause, we can get the same conclusion as represented in section 3.2, although the fundamental frequencies of the cavity mode change as well as the location of the FLRs.

It should be noted that the ULF energy dissipation process is not included in the present numerical model, which is not the case in reality. The energy loss of the ULF waves may be caused by either the wave-particle interaction or the Joule heating in the ionosphere due to the finite Pederson conductivity. In addition, the ULF waves would propagate downtail if we consider the waveguide mode, which would also result in the energy loss of the ULF waves. All these factors would be considered in a more realistic model.

## 5 Conclusions

In this paper, we used the dipole model developed by Lee and Lysak<sup>[31]</sup> to quantitatively investigate the ULF waves excited by the sudden impulse (SI) of the solar wind dynamic pressure interacting with the dipole magnetosphere. The main results are as follows:

(1) For a given impulse lasting for 1 min with amplitude of 50 mV/m and duration of 1 min impinging on the subsolar magnetopause, the total ULF energy transported from the solar wind to

the magnetosphere is about  $1.1 \times 10^{14}$  J. The efficiency of the solar wind energy input is about 1%, which depends little on the location of the magnetopause in the model.

(2) It is demonstrated that the energy of the global cavity mode is confined in the region near the magnetopause, whereas, the energy of the toroidal mode may be distributed among a few specific *L*-shells.

(3) The numerical results here indicate that fundamental frequency of the global cavity mode is identical despite of the spectrum characteristics of the external driving impulse, and the central locations of the FLRs do not vary noticeably either. We believe it is due to the coupling of the cavity modes and the toroidal waves.

(4) The impulse with relatively broad spectrum may excite more harmonics of the cavity mode, which implies that the spectrum of the impulse could prominently affect the excitation of the higher harmonics of the global cavity mode. When the higher harmonics appear, the regions of the FLRs will be broadened. We speculate that more cavity mode harmonics would stimulate the FLRs on more magnetic shells, which will cause the toroidal energy dispersion.

*We are grateful to Heddal for providing the primary numerical code.*

- 1 Allan W, Poulter M E. ULF waves — their relationship to the structure of the Earth's magnetosphere. Reports of Progress in Phys, 1992, 55: 533—598[DOI]
- 2 Dungey J W. Electrodynamics of the outer atmosphere. Phys Ionosphere, 1955, 229
- 3 Chen L, Hasegawa A. A theory of long-period magnetic pulsations, I, Steady state excitation of field line resonance. J Geophys Res, 1974, 79: 1024—1032
- 4 Southwood D J. Some features of field line resonances in the magnetosphere. Planet Space Sci, 1974, 22: 483—491
- 5 Samson J C, Jacobs J A, Rostoker G. Latitude-dependent characteristics of long-period geomagnetic micropulsations. J Geophys Res, 1971, 76: 3675—3683
- 6 Samson J C, Rostoker G. Latitude-dependent characteristics of high-latitude Pc4 and Pc5 micropulsations. J Geophys Res, 1972, 77: 6133—6144
- 7 Kivelson M G, Southwood D J. Resonant ULF waves: A new interpretation. Geophys Res Lett, 1985, 12: 49—52[DOI]
- 8 Kivelson M G, Southwood D J. Coupling of global MHD eigenmodes to field line resonances. J Geophys Res, 1986, 91: 4345—4351[DOI]
- 9 Allan W, White S P, Poulter E M. Impulse-excited hydromagnetic cavity and field-line resonances in the magnetosphere. Planet Space Sci, 1986, 34: 371—385[DOI]
- 10 Inhester B. Numerical modeling of hydromagnetic wave coupling in the magnetosphere. J Geophys Res, 1987, 92: 4751—4756[DOI]
- 11 Zhu X, Kivelson M G. Analytic formulation and quantitative solutions of the coupled ULF wave problem. J Geophys Res, 1988, 93: 8602—8612[DOI]
- 12 Lee D H, Lysak R L. Magnetospheric ULF wave coupling in the dipole model: The impulsive excitation. J Geophys Res, 1989, 94: 17097—17103[DOI]
- 13 Walker A D M, Ruohoniemi J M, Baker M K, et al. Spatial and temporal behavior of ULF pulsations observed by the Goose Bay HF radar. J Geophys Res, 1992, 97: 12187—12202[DOI]
- 14 Samson J C, Harrold B G, Ruohoniemi J M, et al. Field line resonances associated with MHD waveguides in the magnetosphere. Geophys Res Lett, 1992, 19: 441—444[DOI]
- 15 Wright A N. Dispersion and wave coupling in inhomogeneous MHD waveguides. J Geophys Res, 1994, 99: 159—167[DOI]
- 16 Wright A N, Rickard G J. ULF pulsations driven by magnetopause motions: Azimuthal phase characteristics. J Geophys Res, 1995, 100: 23703—23710[DOI]
- 17 Wright A N, Rickard G J. A numerical study of resonant absorption in a magnetohydrodynamic cavity driven by a broad band spectrum. Astrophys J, 1995b, 444: 458—470[DOI]
- 18 Mann I R, Chisham G, Bale S D. Multisatellite and ground-based observations of a tailward propagating Pc5 magnetospheric waveguide mode. J Geophys Res, 1998, 103: 4657—4670[DOI]

- 19 Mann I R, Wright A N, Mills K J, et al. Excitation of magnetospheric waveguide modes by magnetosheath flows. *J Geophys Res*, 1999, 104: 333–353[DOI]
- 20 Stephenson J, Walker A D M. HF radar observations of Pc5 ULF pulsations driven by the solar wind. *Geophys Res Lett*, 2002, 29: 1297, doi:10.1029/2001GL014291
- 21 Kepko L, Spence H E, Singer H J. ULF waves in the solar wind as direct drivers of magnetospheric pulsations. *Geophys Res Lett*, 2002, 29: 1197, doi:10.1029/2001GL014405
- 22 Kepko L, Spence H E. Observations of discrete, global magnetospheric oscillations directly driven by solar wind density variations. *J Geophys Res*, 2003, 108(A6): 1257, doi:10.1029/2002JA009676
- 23 Greenwald R A, Walker A D M. Energetics of long period resonant hydromagnetic waves. *Geophys Res Lett*, 1980, 7: 745–748[DOI]
- 24 Crowley G, Hughes W J, Jones T B. Observational evidence of cavity modes in the Earth's magnetosphere. *J Geophys Res*, 1987, 92: 12233–12240[DOI]
- 25 Rae I J, Donovan E F, Mann I R, et al. Evolution and characteristics of global Pc5 ULF waves during a high solar wind speed interval. *J Geophys Res*, 2005, 110: A12211, doi:10.1029/2005JA011007
- 26 Wang Y F, Fu S Y, Zong Q G, et al. Multi-spacecraft observations of ULF waves during the recovery phase of magnetic storm on October 30, 2003. *Sci China Ser E-Tech Sci*, 2008, 51(10): 1772–1785
- 27 Hughes W J. The effect of the atmosphere and ionosphere on long period magnetospheric micropulsations. *Planet Space Sci*, 1974, 22: 1157–1172
- 28 Hughes W J, Southwood D J. The screening of micropulsation signals by the atmosphere and ionosphere. *J Geophys Res*, 1976, 81: 3234–3247
- 29 Elkington S R, Hudson M K, Chan A A. Acceleration of relativistic electron via drift-resonant interaction with toroidal-mode Pc-5 ulf oscillations. *Geophys Res Lett*, 1999, 26: 3273–3276[DOI]
- 30 Zong Q G, Zhou X Z, Li X, et al. Ultralow frequency modulation of energetic particles in the dayside magnetosphere. *Geophys Res Lett*, 2007, 34: L12,105[DOI]
- 31 Lee D H, Lysak R L. Monochromatic ULF wave excitation in the dipole magnetosphere. *J Geophys Res*, 1991, 96: 5811–5817[DOI]
- 32 Singer H J, Southwood D J, Walker R J, et al. Alfvén wave resonances in a realistic magnetospheric magnetic field geometry. *J Geophys Res*, 1981, 86: 4589–4596[DOI]
- 33 Hededal C B. A numerical dipole model of the Earth's Magnetosphere. Master Thesis. Copenhagen: University of Copenhagen, 2001
- 34 Tanskanen E, Pulkkinen T I, Koskinen H E J, et al. Substorm energy budget during low and high solar activity: 1997 and 1999 compared. *J Geophys Res*, 2002, 107(A6): 1086, doi:10.1029/2001JA900153
- 35 Wygant J, Mozer F, Temerin M, et al. Large amplitude electric and magnetic field signatures in the inner magnetosphere during injection of 15 MeV electron drift echoes. *Geophys Res Lett*, 1994, 21: 1739–1742[DOI]
- 36 Goldstein J, Hudson M K, Lotko W. Possible evidence of damped cavity mode oscillations stimulated by the January 1997 magnetic cloud event. *Geophys Res Lett*, 1999, 26: 3589–3592[DOI]
- 37 Eriksson P T I, Blomberg L G, Schaefer S, et al. On the excitation of ULF waves by solar wind pressure enhancements. *Ann Geophys*, 2006, 24: 3161–3172
- 38 Lee D H, Kim K H, Denton R E, et al. Effects of ionospheric damping on MHD wave mode structure. *Planet Space Sci*, 2004, 56: e33–e36